

Comparison of machine learning algorithms for classification of LiDAR points for characterization of canola canopy structure

Lian Wu, Xuan Zhu, Roger Lawes, David Dunkerley & Heping Zhang

To cite this article: Lian Wu, Xuan Zhu, Roger Lawes, David Dunkerley & Heping Zhang (2019): Comparison of machine learning algorithms for classification of LiDAR points for characterization of canola canopy structure, International Journal of Remote Sensing, DOI: [10.1080/01431161.2019.1584929](https://doi.org/10.1080/01431161.2019.1584929)

To link to this article: <https://doi.org/10.1080/01431161.2019.1584929>



Published online: 27 Feb 2019.




Submit your article to this journal [↗](#)



View Crossmark data [↗](#)



Comparison of machine learning algorithms for classification of LiDAR points for characterization of canola canopy structure

Lian Wu ^a, Xuan Zhu^a, Roger Lawes^b, David Dunkerley^a and Heping Zhang^b

^aSchool of Earth, Atmosphere and Environment, Monash University, Clayton, Australia; ^bCSIRO Centre for Environment & Life Sciences, Perth, Australia

ABSTRACT

Recent changes to plant architectural traits that influence the canopy have produced high yielding cultivars in rice, wheat and maize. In breeding programs, rapid assessments of the crop canopy and other structural traits are needed to facilitate the development of advanced cultivars in other crops such as Canola. LiDAR has the potential to provide insights into plant structural traits such as canopy height, aboveground biomass, and light penetration. These parameters all rely heavily on classifying LiDAR returns as ground or vegetation as they rely on the number of ground returns and the number of vegetation returns. The aim of this study is to propose a point classification method for canola using machine learning approach. The training and testing datasets were clusters sampled from field plots for flower, plant and ground. The supervised learning algorithms chosen are Decision Tree, Random Forest, Support Vector Machine, and Naïve Bayes. K-means Clustering was also used as an unsupervised learning algorithm. The results show that Random Forest models (error rate = 0.006%) are the most accurate to use for canola point classification, followed by Support Vector Machine (0.028%) and Decision Tree (0.169%). Naïve Bayes (2.079%) and K-means Clustering (48.806%) are not suitable for this purpose. This method provides the true ground and canopy in point clouds rather than determining ground points via a fixed height rely on the accuracy of the point clouds, subsequently gives more representative measurements of the crop canopy.

ARTICLE HISTORY

Received 5 November 2018
Accepted 14 January 2019

1. Introduction

Canopy structure affects the microclimatic conditions within the crop canopy such as sunlight, humidity, temperature, contact frequency, as well as light transmittance and attenuation (Pangga, Hanan, and Chakraborty 2013; Sankaran, Khot, and Carter 2015; Costes et al. 2013). These factors then influence the nitrogen status and photosynthetic and transpiration activities of plants and potentially the risk of disease infection and lodging. They ultimately have the ability to affect the crop yield in wheat, rice and maize

(Maddonni, Otegui, and Cirilo 2001; Wu et al. 2014; Omasa, Hosoi, and Konishi 2006; Hua et al. 2016). The following studies have examined the dynamics of crop traits by modifying the canopy structure. Maddonni, Otegui, and Cirilo (2001) suggested that modifying shoot size and leaf orientation may cause shade avoidance reactions. Hua et al. (2016) demonstrated the potential of increasing crop yield by decreasing the tiller angle and leaf inclination angle of the rice plants. In contrast, sparse canopies may lower the incidence and reduce the severity of the disease (Wu et al. 2014). However, a sparse canopy can limit the biomass production and consequently lower the crop yield, meaning that the balance between disease management and crop yield needs to be considered carefully in order to have the best outcome possible (Wu et al. 2014). These case studies emphasize the effects and importance of canopy structure on crop growth and highlight the significance of studying and quantifying canopy structure to increase crop yield. Recent changes to plant architectural traits that influence the canopy have produced high yielding cultivars in rice, wheat and maize. In breeding programs, rapid assessments of the crop canopy and other structural traits are needed to facilitate the development of advanced cultivars in other crops such as Canola (*Brassica napus*). The morphology of canola is different from those of rice, wheat and maize in many ways. The most noticeable differences are the leaf shape, leaf size, and the flower colour (Colton and Sykes 1992), which are useful in developing specific methodologies for estimating canola canopy structural parameters.

Light Detection and Ranging (LiDAR) is one of the most well-known and widely deployed remote sensing technique for generating canopy models (2-dimentional and 3-dimentional) for extracting canopy structural information and characterizing crop traits (Koenig et al. 2015). LiDAR directly measures the distance between the sensor and the target object by calculating the elapsed time between the emission and the returns and then produces point clouds. Ground-based platforms are often used in preference to airborne systems for crops, as the general accuracy of airborne LiDAR is around 0.1–1 m while that of ground-based LiDAR is 0.05–10 cm (Omasa, Hosoi, and Konishi 2006; Deery et al. 2014; Jimenez-Berni et al. 2018). Generally, canopy structural information such as canopy height, light penetration index, leaf area index, above ground biomass, and fractional ground cover, can be extracted from LiDAR data using two different approaches. One involves signal/image processing and pattern recognition (Jimenez-Berni et al. 2018; Friedli et al. 2016; McMahon et al. 2015; Raunonen et al. 2013) and the other relies on statistical analysis for correlations and predictions (Nie et al. 2016; Li et al. 2015; Cui et al. 2011; Zhao et al. 2011; Korhonen et al. 2011; Richardson, Moskal, and Kim 2009; Lim et al. 2003; Lefsky et al. 2002; Calders et al. 2015; Zhao et al. 2015). The first approach extracts and measures LiDAR metrics directly from point clouds, though canopy structural parameters, such as above ground biomass, leaf area index, light attenuation and canopy volume, are impossible to be extracted directly from LiDAR data (Li et al. 2015; Calders et al. 2015; Nie et al. 2016; Korhonen et al. 2011; Richardson, Moskal, and Kim 2009; Maddonni, Otegui, and Cirilo 2001; Cui et al. 2011; Lim et al. 2003). Instead, they need to be derived by methods involving allometric relationships with LiDAR metrics that can be derived directly from point clouds such as canopy height.

Among all of the canopy structural parameters derived from LiDAR, canopy height, above ground biomass, and light penetration index are most affected by the accuracy

and efficiency of the LiDAR point classification. Canopy height is one of the most common canopy structural parameters for both crops and forest as it indicates the crop performance and health (Friedli et al. 2016). Crop canopy height obtained from LiDAR point clouds has been approached differently in published papers. Li et al. (2015) used the average height of the entire LiDAR point clouds as the canopy height. Deery et al. (2014) took canopy height measurement as the mean of the top 95th percentile of the point cloud height distribution after subtracting the ground elevation. Similarly, Jimenez-Berni et al. (2018) measured canopy height as the difference between the ground, which was taken as the bottom 2% of the points in the point cloud and the top 3% of the points. However, these methodologies tend to use a fixed percentile when measuring canopy height, which turns the height of the actual canopy into those of the point cloud, thus it is necessary to recognize the true ground and plants from the point clouds.

Above ground biomass (AGB) is another major canopy parameter as it contains biophysical information, productivity, and carbon storage of vegetation (Calders et al. 2015; Li et al. 2015). Also, biomass in canola is highly associated with the final yield (Aminpanah 2013), thus having accurate non-destructive biomass estimate can improve the reliability and accuracy of canola yield estimation. Unlike canopy height, AGB cannot be measured directly from any of the attributes of LiDAR data. Instead, an allometric relationship with metrics that can be derived from LiDAR attributes is established. For instance, Li et al. (2015) correlated AGB with the mean of canopy height, the variation of canopy height, NDVI and LiDAR penetration index (LPI). Their results suggested that the mean of canopy height has the strongest correlation with AGB. Jimenez-Berni et al. (2018) proposed two ways of accessing AGB from LiDAR point clouds. They are voxel-based and profile-based approaches. Nevertheless, they are both associated with the height of each point.

Light penetration is not only useful for measuring AGB but also essential for leaf area index (LAI) estimation. Previous studies have assessed crop LAI based on the Beer-Lambert law for light interception, which is formulated as Equation (1):

$$I = I_0 \exp(-k(\text{LAI})) \quad (1)$$

where I_0 is irradiance above the canopy, I is irradiance beneath the canopy, and k is the extinction coefficient (Solberg et al. 2006; Li et al. 2015; Nie et al. 2016). However, substituting light attenuation I/I_0 with LiDAR metrics is necessary when estimating LAI with LiDAR point cloud attributes. Hence, the ratio of the number of ground returns (N_{ground}) to the sum of ground and vegetation returns ($N_{\text{ground}} + N_{\text{vegetation}}$) is applied as the light attenuation, which is given by Equation (2):

$$\text{LPI} = \frac{N_{\text{ground}}}{N_{\text{ground}} + N_{\text{vegetation}}} \quad (2)$$

this ratio is known as light penetration index (LPI). Subsequently, LAI estimation with LiDAR data can be expressed as Equation (3) (Nie et al. 2016):

$$\text{LAI} = -\frac{\ln(\text{LPI})}{k} \quad (3)$$

Cui et al. (2011) estimated corn LAI based on the gap fraction of the canopy expressed as Equation (4):

$$\text{LAI} = -\frac{\ln(f_{\text{gap}})}{\lambda_0 \times G} \mu \quad (4)$$

where f_{gap} is the gap fraction, λ_0 is the Nilson parameter, G is the mean projection of a unit of leaf area, and μ is the cosine of the zenith angle. Li et al. (2015) also built a relation between LAI and one of the metrics they accessed and results showed that LAI correlated with NDVI the most.

The canopy structural parameters mentioned above rely heavily on the classification of LiDAR returns into ground and plant as they associate the number of ground returns and the number of vegetation returns. The majority of the published methodologies on ground determination are based on either the intensity information or the height of LiDAR points. LiDAR intensity information can be used to differentiate the ground and green vegetation because a greater proportion of the laser gets absorbed by vegetation than ground (Jimenez-Berni et al. 2018; Liu et al. 2017). This method has been implemented on wheat, which has a relatively uniform colour throughout the entire plant. However, it would not be the case for crops like canola that has different colour flowers near the top of the LiDAR point cloud when maturing. Using the height frequency distribution only for recognizing ground returns from the LiDAR point cloud may not be appropriate for early growth stages when the plants are still very close to the ground (Jimenez-Berni et al. 2018; Friedli et al. 2016; Koenig et al. 2015). Studies also used software *TerraScan* built-in function to separate ground returns but major manual reclassification is required as the software gives a significant number of misclassified points, which subsequently leads to errors in the result (Nie et al. 2016; Luo et al. 2014; Cui et al. 2011). Therefore, a better ground-level determination and point classification method is needed for canola and crops at early growth stages.

This paper aims to evaluate machine learning techniques as alternative methods to improve the accuracy of LiDAR point classification of ground and different parts of canola plants. We compared five machine learning algorithms with training datasets that are built specifically to characterize different plant parts in LiDAR point clouds, which include Decision Tree, Naïve Bayes, K -mean clustering, Random Forest, and Support Vector Machines (Alexander et al. 2010; Gerke and Xiao 2014; Pal and Mather 2003; Ducic et al. 2006; Rutzinger et al. 2008; Zlinszky et al. 2012; Koenig et al. 2015, 2013; Lindberg et al. 2013; Elshkaki et al. 2005; Vauhkonen et al. 2012; Liu et al. 2017). These methodologies cope with categories within the 3D point clouds differently, and the methodology is likely to affect the ability to reliably estimate ABG, LPI and canopy height. More precise estimate of crop attributes would enable researchers to better identify which traits meaningfully impact on crop yield, and we explore this question herein.

2. Methodology

2.1. Field experiment

The LiDAR data were captured in a trial farm located in Kojonup (33°52'S; 116°43'E), Western Australia. LiDAR was run on 6th September, 2017 over 10 different plots. LiDAR

Table 1. LiDAR specifications.

Feature	Value
Light source wavelength (nm)	650 (visible red light)
Aperture angle (°)	70
Scanning frequency (Hz)	300
Angular resolution (°)	0.1
Operation range (m)	0.7–3

sensor selected to capture the canola canopy structure was SICK LMS400-2000, which operates at visible red light of approximately 650 nm (Table 1). LiDAR was mounted on a portable ground-based platform, Phenomobile (Figure 1). The adjustable wheelbase and boom allow Phenomobile to adapt to different plot widths and crop species, in order to keep the distance between the canopy top and the sensor constant as crop grows. Then, the Phenomobile was pushed along the plot to finish the scanning. For detailed descriptions about Phenomobile refer to Deery et al. (2014) and Jimenez-Berni et al. (2018).

This dataset contains canola plots that can be roughly categorized into two growth stages, which are mature and young (detailed in Table 2). The raw LiDAR data was then uploaded to *PhenoSMART*, which is a software that is under development by Commonwealth Scientific and Industrial Research Organisation (CSIRO), for LiDAR data processing.

2.2. Data pre-processing

PhenoSMART is a web-based application that allows users to manipulate data easily by gathering raw LiDAR data and the corresponding GPS to construct geocoded point cloud in 3D for each plot uploaded. The coordinates of points (XYZ) are truncated to the location of each returns in relation to the LiDAR sensor in millimetre. As the



Figure 1. LiDAR sensor mounted on Phenomobile, highlighted with red box. Photo taken in Kojonup (33°52'S; 116°43'E).

Table 2. Ten canola plots with growth stage and the total number of points in each point cloud. The total number of points selected for training purpose is at least 1.77% of the total number of points in each point cloud.

Plot no.	Growth stage	Total number of points in LiDAR point cloud	Total number of points in clusters for training and testing	Proportion of total as training dataset (%)
01	Mature	665 066	14 187	2.13
02	Mature	657 716	16 381	2.49
04	Mature	954 417	16 897	1.77
08	Mature	1 085 461	29 365	2.71
10	Mature	1 309 982	29 632	2.26
03	Young	675 999	37 615	5.56
05	Young	772 776	29 888	3.87
06	Young	658 954	17 370	2.64
07	Young	545 893	17 056	3.12
0	Young	719 303	16 333	2.27

location of LiDAR sensor is set to be zero, therefore any point located beneath the LiDAR has negative Z value. Then, it applies an outlier removal filter to point clouds. Users then select and crop the area of interest out of the point cloud. Features estimated from the area of interest are the canopy height, fractional ground cover, and biomass. Detailed methodologies on *PhenoSMART* refer to Jimenez-Berni et al. (2018).

2.3. Reference data acquisition

CloudCompare (<https://www.cloudcompare.org/2018>) was used to visualize point clouds processed by *PhenoSMART*. Three different classes for mature canola point clouds were identified visually, namely ground, plant, and flower. Younger canopies had not yet flowered, and had only ground and plant returns. From each mature canopy plot, 20 flower clusters, 10 ground clusters, and 5 plant clusters were sampled. Young canopy plots have 10 ground clusters and 5 plant clusters. Subsequently, all of the clusters sampled from mature canopy point clouds were collected to build a mature model while the clusters from young canopy point clouds were assembled to construct a young model. These clusters were carefully selected from the point clouds. Although the total number of selected points from each plot varies depending on the size of clusters, each representative cluster contained at least 1,000 training cases (points) in order to build comprehensive and demonstrative models.

Ground clusters were picked in the areas where there were no plants growing on top, meaning that the LiDAR reached to the surface of the ground directly as shown in [Figure 2\(a\)](#). Flower clusters in mature canopy plots were recognized by height and the intensity as flowers are likely to be near the top of the canopy and the intensity of flower returns are usually significantly higher than plant returns due to the yellow colour ([Figure 2\(b\)](#)). Also, the flower clusters should retain the shape of circle when viewing from top-down as flowers grow around the stem. Plant clusters were selected as the points located in the middle of the point cloud with relatively lower intensity value than flower returns. The selection of clusters avoided confusion areas where different types of points can co-exist and the accuracy of the clusters was re-ensured by examining the shape of the cluster to make sure that they belong to their corresponding class.

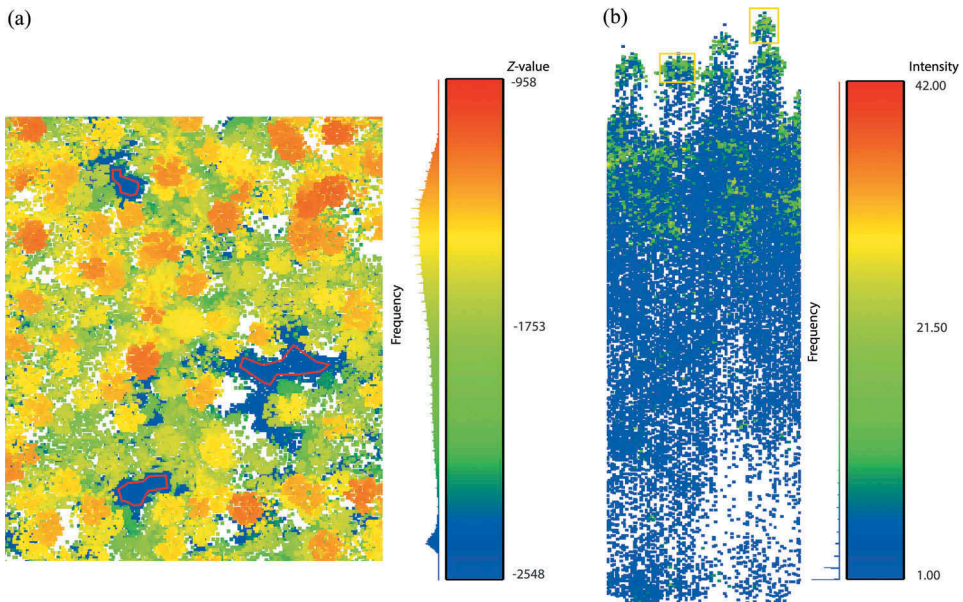


Figure 2. Example of clusters extraction from point clouds as training dataset for ground in top-down view of height (a) and flower in side-view of intensity (b). Ground clusters are circled in red and an example of a cluster of flower returns is highlighted with yellow box.

2.4. Machine learning algorithms

The algorithms included both supervised and unsupervised algorithms (i.e. *K*-mean clustering), as well as meta-learning algorithms (i.e. random forest).

Supervised learning algorithms are given the target classes and clear instruction for what to learn. In other words, these algorithms build models knowing the answers (Ghatak 2017). In this study, the target class is manually classified LiDAR points and four different supervised learning algorithms were chosen. Decision Tree (DT) is one of the most popular machine learning classifiers to be used in studies, as it requires no extra parameter for model construction. The DT model is constructed by a heuristic called recursive partitioning, which repeatedly subsets the dataset until one terminating condition is reached and the terminated subset is homogeneous (Hansen, Dubayah, and Defries 1996). Random Forest (RF) is a meta-learning algorithm, which focuses on improving learning steps based on the results of other learning algorithms. It is called forest as it literally involves numerous tree models (Breiman 2001). Once a number of DT models are built, voting takes place to combine the results of the DT models. Naïve Bayes (NB) is a supervised learning algorithm that relies on the likelihood of potential outcomes. However, it is called naïve because it simply assumes all input features in training dataset are equally important (Lantz 2015). Support Vector Machines (SVM) is another supervised learning algorithm that constructs relationship between input and output via plotting the data in a multidimensional manner. Then, SVM creates boundaries called hyperplanes, which separate the space in the plot to create homogeneous subset of the data. Ideally, the hyperplanes divide the dataset into smaller subsets that are homogeneous. (Lantz 2015; Koenig et al. 2015; Hansen, Dubayah, and Defries 1996; Ghatak 2017)

Unsupervised learning uses an unlabelled training dataset, meaning it requires no manually pre-defined data. The learning type finds the pattern to discriminate different classes in the dataset by itself. *K*-means clustering is one of unsupervised learning algorithms (Zhao et al. 2018). However, prior knowledge about the number of clusters wanted is required. Then, the aim of *K*-means clustering algorithms is to maximize the differences between the clusters defined and minimize the differences within each cluster at the same time. In this study, *k* value was set to be two for young canopy and three for mature canopy as flower, plant, and ground.

In order to build training and testing datasets for supervised learning algorithms, 70% of the points in sampling dataset was used for training models and the other 30% was used to build confusion matrix and to assess the accuracy of the models. In both of the datasets for model construction, each point has five attributes, which are its coordinates (XYZ), intensity value, and its corresponding class, i.e. either ground, plant or flower. In the Equations (5) and (6), TP (true positive) is the points that are correctly classified as the class of interest, TN (true negatives) the points classified correctly as not the class of interest, FP (false positives) the points classified incorrectly as the class of interest, and FN (false negatives) the points classified incorrectly as not the class of interest (Lantz 2015).

$$\text{Accuracy} = \frac{\text{TP} + \text{TN}}{\text{TP} + \text{TN} + \text{FP} + \text{FN}} \quad (5)$$

$$\text{Errorrate} = 1 - \text{Accuracy} \quad (6)$$

The overall workflow is illustrated in Figure 3.

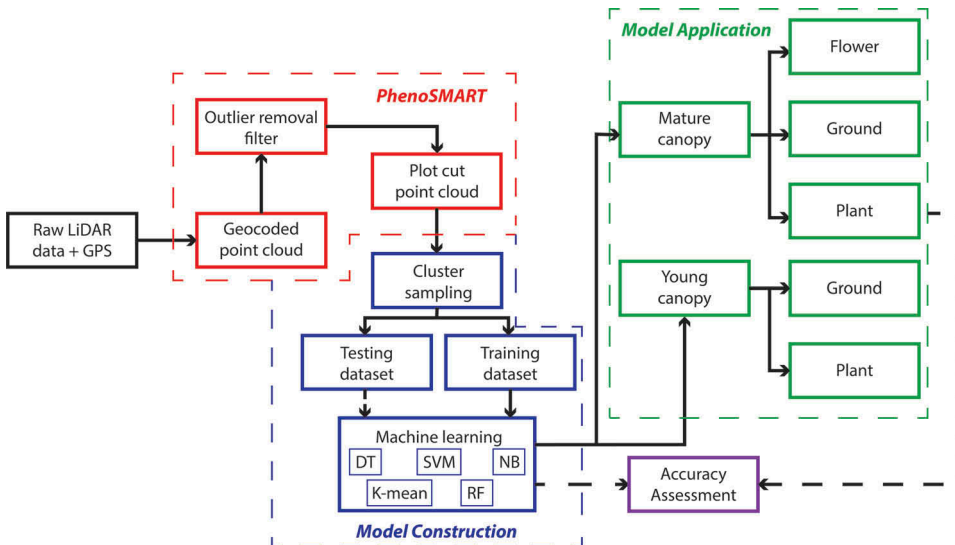


Figure 3. Overall workflow.

3. Results

3.1. Classification via machine learning

3.1.1. Supervised learning algorithms

The DT algorithm used only height information (Z value of -2303) for constructing young model and had two terminal nodes, namely ground and plant. The DT young model had no misclassified points for the young training dataset. On the other hand, the DT algorithm used height information and intensity in tree construction and had four terminal nodes rather than three. As shown in Figure 4, mature model used intensity and then applied height information to differentiate ground and flower returns. Plant class appeared in both of the second layer branches, meaning that height was the only criterion for plant returns. The benchmark for intensity used in the mature model was 11.5 , meaning that points were split into two branches, the one with high intensity contained possible flower and plant points while the other branch included possible ground and plant points. Then, height criterion was applied to confirm the actual class of these possible points, which those located beneath -2345 along the Z axis in the lower intensity branch were classified as ground and the points located above that benchmark were then recognized as plant. Similarly, the possible points located above Z value of -1830 in the high-intensity branch were put into the flower class and the others into the plant class.

In the RF young model, the error rate of plant class remained constant from plotting 1 tree to 500 trees. Conversely, the error rate of ground class increased drastically in the

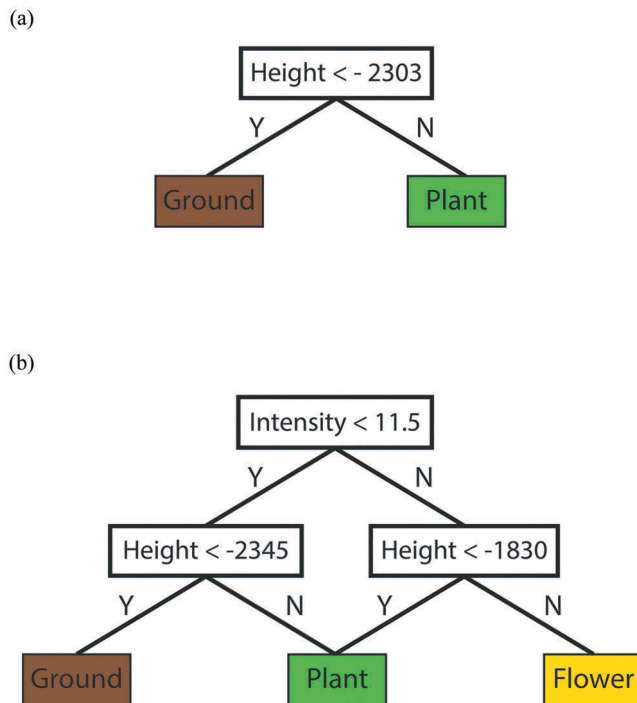


Figure 4. Tree structure for decision tree young (a) and mature (b) models.

first 10 trees and dropped back to zero then remained stable like the plant class. The overall error rate of the RF young model for the young training dataset was zero. In a more complicated case, the error rates of all three classes in RF mature model fluctuated within the first 250 trees, especially in the first 50 trees where the error rates of three classes all reached their peaks and reduced back to a relatively low error rate. However, the error rate of ground class peaked within the first 30 trees and remained at its peak for the rest of the trees without decreasing the error rate like the others. Plant class had the lowest error rate in both young and mature models. Other than the ground class in mature model, the error rate decreased and became stable as the number of trees increased. Figure 5 shows the results of RF.

Figure 6 visualizes both of the SVM models and indicates points and the support vectors, which are the points located near the hyperplanes the model plotted to separate different classes. In the young model, most of the points were within their corresponding boundaries but some of the ground points with intensity of 12 and above were put into the plant class and some of the plant points located near the ground appeared within the ground boundary. The boundaries of SVM mature models were not as clear as the young model as some of the points overlapped along the hyperplanes.

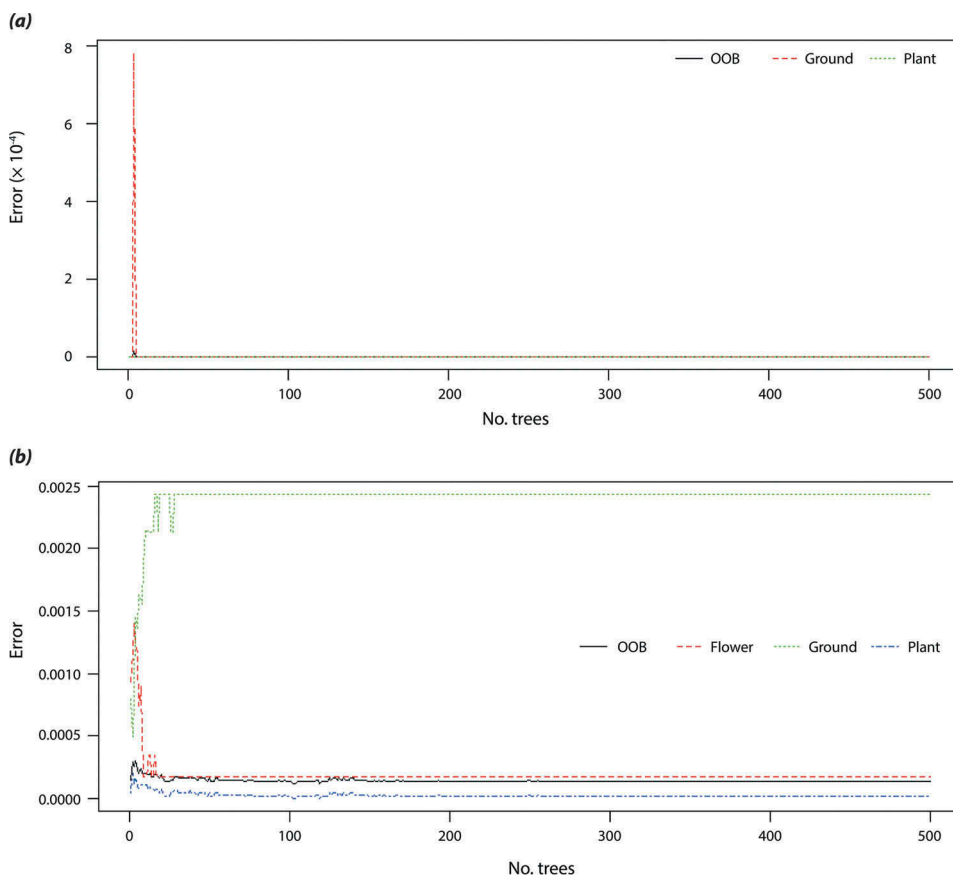


Figure 5. Results of Random Forest models, young model (a) and mature model (b). OOB is the out-of-bag estimate of error rate.

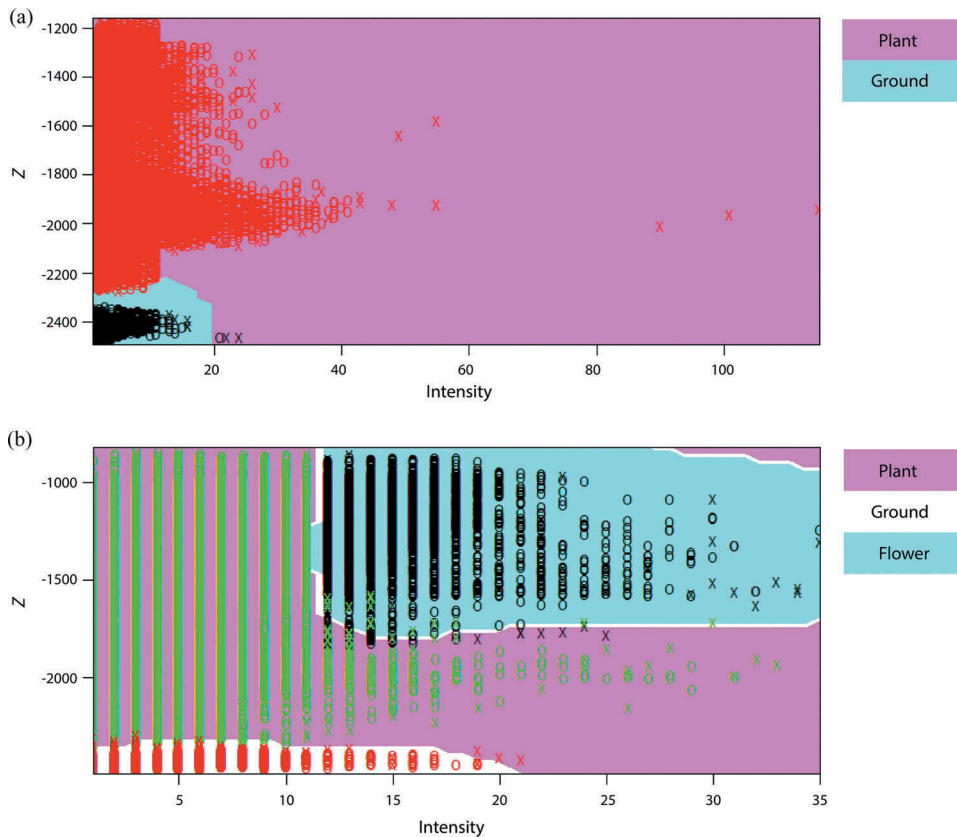


Figure 6. SVM classification plots, young SVM model (a) and mature SVM model (b). Points that are represented by an 'x' are the support vectors while those are represented by 'o' are the other points. For models with three classes, flower points are in black, ground in red, and plant in green. For those with only two classes, ground points are in black and plant in red. The background colours represent the features of the original training data.

Especially with the plant points got misclassified as flower and vice versa along the flower and plant boundary. However, the intensity benchmark for flower points was at around 12, which was consistent with the DT mature model, which used 11.5. The mature model also had the same issue where the ground points with intensity higher than 12 were classified as plant.

3.1.2. Unsupervised learning algorithms

K-means clustering algorithms construct models without predefined classes, though the separation of clusters can still be validated based on the size and the centre features of each cluster (Table 3). However, none of the K-means models demonstrated cluster sizes that were close to the expected size. For example, K-means mature model had three clusters with a similar size whereas one of the clusters should be much larger than the other two as plant class, which was the majority of a canopy. Between-ss/totals (BSS/TSS) is the ratio of the between-cluster sum of squares to the total sum of squares and it was implemented in this study as a measure of the goodness of the K-means clustering.

Table 3. Features of *K*-means clustering centres, including the *Z* value, intensity, and the total number of point for each cluster. Along with the betweenss/totals (BSS/TSS) for each cluster. The order of the clusters is based on the number of the point.

Model	K-means Clusters				BSS/TSS (%)
	Centre	No. of points	Z value	Intensity	
Young	#1 – plant	16 596	–1534.56	3.95	63.3
	#2 – ground	66 187	–1943.64	4.16	
Mature	#1 – ground	18 065	–2122.97	3.10	84.1
	#2 – flower	26 692	–1276.97	6.90	
	#3 – plant	29 766	–1760.75	2.77	

Mature model showed a larger BTT/TSS ratio than the young model, which were 84.1% to 63.3%, respectively. In comparison with other supervised learning mature models, one of the clusters should have a significantly larger size than the others as plant cluster. While the cluster with the lowest *Z* value (i.e. #1) should be the ground cluster, meaning that the other two ought to be either flower or plant, yet they were fairly similar in size and the differences in intensity value among clusters were not significant to tell them apart as flower cluster should be intensity higher than just 6.9. In this case, using *Z* value to differentiate the remaining clusters seemed to be the most reasonable. Cluster #2 had the highest *Z* value compared to #3, thus #2 could be the flower cluster. Conversely, the young model had two clusters that were also similar in size and intensity value; hence, *Z* value should be used again to determine the clusters. To conclude, both young and mature models tend to apply only *Z* value to determine different clusters rather than using height information and intensity together like supervised learning algorithms.

3.2. Accuracy assessment

All of the models were then tested by the testing dataset for assessing the error rates and the confusion matrices (Table 4). There was no interchange between flower and ground classes and no misclassification in RF, SVM and DT young models. RF mature model was the most accurate model for mature canopies out of the other algorithms as it had only two misclassified points. Following by SVM model, which contained 9

Table 4. Modified confusion matrix for supervised learning models via testing dataset. It summarizes the number of misclassified points and the predicted class that they have been put into and therefore the error rate for each model.

Actual class	Plant		Plant		Error rate (%)
	Flower	Ground	Flower	Ground	
Predicted class					
RF young	–	0	–	0	0.000
RF mature	1	0	1	0	0.006
SVM young	–	0	–	0	0.000
SVM mature	7	1	1	0	0.028
DT young	–	0	–	0	0.000
DT mature	16	0	0	38	0.169
NB young	–	255	–	31	0.806
NB mature	598	12	28	26	2.079
K-means young	–	27 917	–	0	78.686
K-means mature	9 145	6 275	168	0	48.806

misclassified points. With a more complex tree structure and more terminal nodes compared to the DT young model, DT mature model had misclassification error rate of 0.169% for testing dataset. The error rate for NB young model was close to 1% while for NB mature model was approximately 2%. Generally, young models tended to be more accurate than mature models as there were only two classes for young canopies. On the contrary, the error rate of *K*-means young model was as high as 79% and it was even higher than its mature model. The reason behind this low accuracy was the number of plant returns that were classified as ground returns incorrectly. While the plant points that were misclassified as flower and ground returns are the main cause for the high error rate of mature model.

3.3. Model application

The models were then applied to the canola canopies after assessing the accuracy of each model and also visualized to examine the applicability and the performance of models when they were applied to actual canola canopy point clouds. RF models as the most accurate, the *Z* value benchmarks of ground class in mature canopies ranged from -2295 to -2328, while the benchmarks used for young canopies are either -2298 or -2303. The flower points RF mature model picked up were the ones with intensity value greater than 12 while the plant points existed throughout the canopy with no specific intensity benchmark. SVM models utilized *Z* value benchmarks ranged larger than the one RF models used, varying from -2199 to -2264 for mature canopies and from -2165 to -2190 for young canopies, which were also higher in elevation than RF models. This resulted in a larger number of ground points classified by SVM models. However, this difference in height benchmarks had a more profound effect on young than mature canopies when modelling using SVM. SVM models also tended to classify ground and plant points in the same areas near the ground level, meaning that these two classes were coexisting in those particular regions. DT models gave very similar classified point clouds to RF models, the most noticeable difference was that the height and intensity benchmarks. The *Z* value benchmark DT models used -2303 for young canopies and -2346 for mature canopies and remained the same in all of the plots. Also, the intensity benchmark for ground class (i.e. 11) stayed the same in all of the mature canopies. In terms of flower classification, the results were fairly similar for RF, SVM and DT models. Though, the flower points recognized by SVM and DT models tended to go lower in the point cloud compared to the RF model. The circle shape for flowers was more evident using the RF model.

The accuracy of NB and *K*-means models was significantly lower than the others as assessed by testing dataset. NB models for both young and mature canopies had classified ground points near the top of the canopy and the benchmark of ground class was the lowest in elevation compared to other algorithms. Especially in the mature plots, only the ground points located in the middle of the point clouds were classified as ground returns rather than randomly scattered near the ground level in a point cloud. *K*-means models classified points based on solely the height information, causing the number of ground and flower returns to be too large while the number of plant points was significantly lower than expected (e.g. [Figure 7](#) for young canopy example and [Figure 8](#) for mature canopy example).

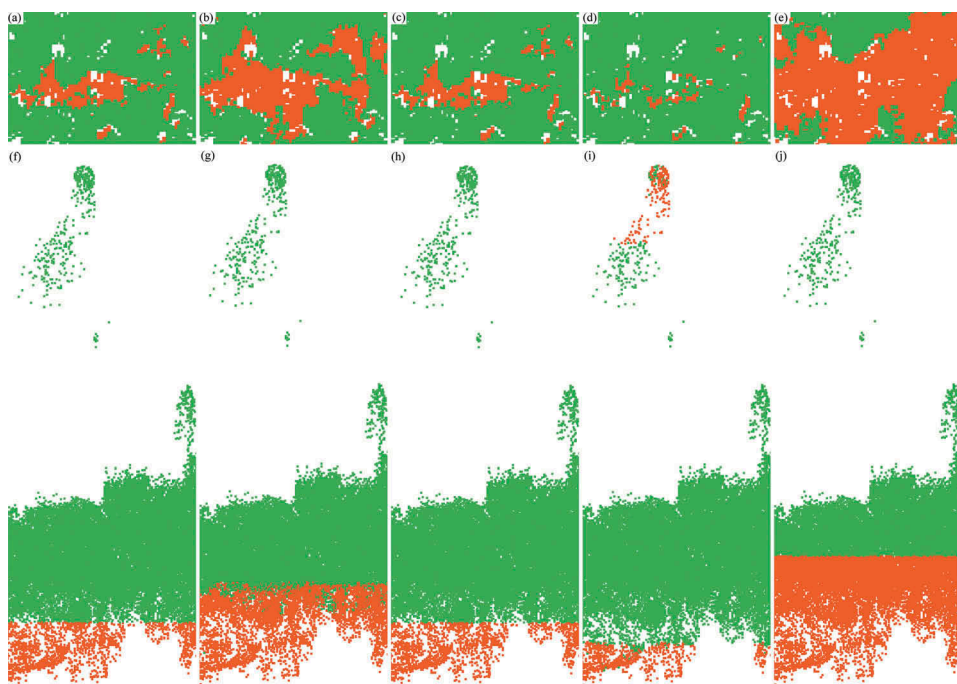


Figure 7. Comparisons of the young model results for RF (a and f), SVM (b and g), DT (c and h), NB (d and i), and *K*-means clustering (e and j) algorithms. Examples shown are top-down view and side view of plot 03. Plant and ground points are in green and orange, respectively. Ranged in order of their accuracy.

4. Discussion and conclusions

In this study, five different machine learning algorithms were examined for canola point cloud classification. The selection includes four different supervised learning algorithms (RF, SVM, DT, and NB) and one unsupervised algorithm (*K*-means clustering), then the accuracy of each of them was assessed and compared.

RF as one of the supervised algorithms applied, its results show the highest accuracy compared to others. When applying RF models to the actual canola point clouds, the benchmarks were customized in different plots rather than using the same benchmarks for plots like DT models. DT as the basic building component of RF, on the other hand, the DT young and mature models apply the same benchmark for the corresponding canopies. This fundamental difference leads to a lower accuracy for DT models compared to RF and even SVM. The tree structure of DT mature model is more complex containing one more layer of criteria and two more terminal nodes, leading to a higher error rate compared to its young model. The SVM young model has 0% error rate, though when it applied to young canopies it tends to classify more ground points compared to RF and DT young models, which both have 0% error rate. Similarly to RF, SVM models also use customized benchmarks in different plots, making more accurate models in general compared to DT models. NB is the only supervised learning algorithm used that does not have 0% error rate for its young model. NB models tend to misclassify points near the top of the canopy as ground points for both young and

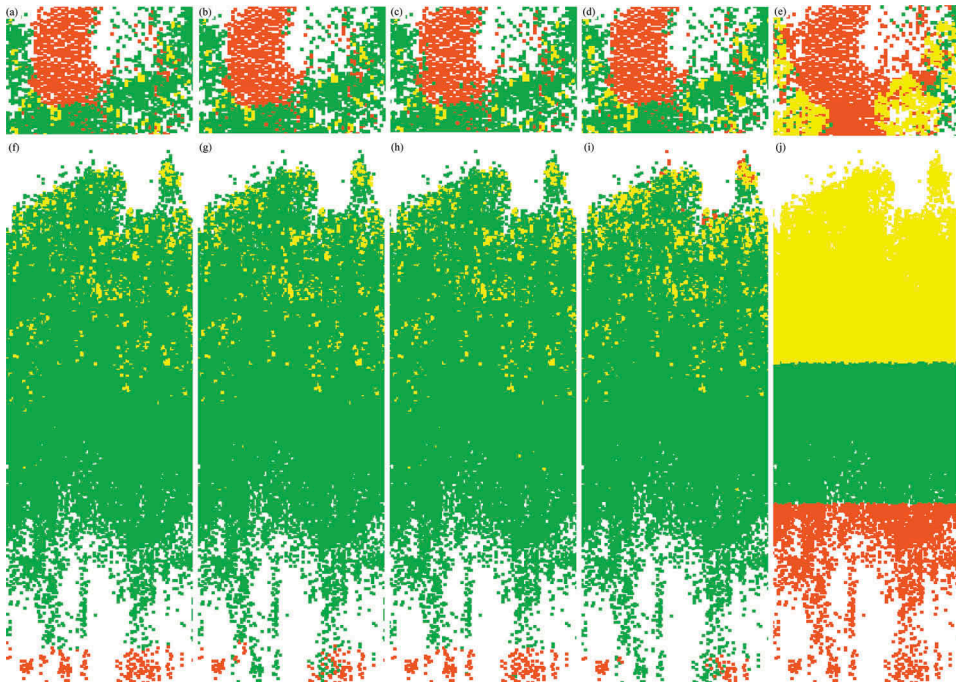


Figure 8. Comparisons of the mature model results for RF (a and f), SVM (b and g), DT (c and h), NB (d and i), and *K*-means clustering (e and j) algorithms. Example shown is top-down view and side view of plot 10. Flower, plant and ground points are in bright yellow, green and orange, respectively.

mature canopies, also it only recognizes ground returns that are located near the centre of the point clouds. Thus, NB algorithm not suitable for canola point classification.

The only unsupervised algorithm used in this study, *K*-mean clustering, is inadequate to be used for point classification as it failed to segment the point clouds into classes that are distinct enough to label. The classification would not make sense if height information is the only criterion used to classify the points.

RF, SVM, and DT all show potential to be used as a model for point classification. Although SVM and DT models show relatively high accuracy, they are still not the most suitable for canola point classification compared to RF. As SVM models tend to have plant and ground points coexisting in the areas near the ground and DT uses benchmarks that are not customized for individual plots. Therefore, RF models are the most suitable to use for canola point classification regardless of the growth stage. This result is supported by the findings of Koenig et al. (2015), which compared the performance of DT, RF, NB, and *K*-means algorithms for post-harvest growth detection and supervised algorithms (i.e. DT, RF and NB) all gave fairly similar post-harvest growth coverage, which was closer to the RGB-image analysis than *K*-means that doubled the post-harvest growth coverage. One of the major differences between this study and Koenig et al. (2015) is that this study involves three target groups for mature canopy. Another major difference is that Koenig et al. (2015) used pre-existing geometric and radiometric

criteria to build a training dataset while the training dataset of this study was built by selecting the true ground and plant parts from LiDAR point clouds.

In conclusion, this study focused on point classification for canola canopy captured using LiDAR and the main findings are: (1) LiDAR can be used to differentiate plant parts; (2) both height and intensity information derived from LiDAR point cloud need to be considered when identifying canola plant traits; (3) supervised classifiers generally perform better than unsupervised one with canola point cloud; and (4) Random Forest performs the best in canola point classification compared to other algorithms used in this study regardless of the growth stage. This method provides the true ground and canopy in point clouds rather than determining ground points via a fixed height percentile in point clouds. Meaning that the canopy structural parameters that heavily rely on the accuracy of the point classification are estimated directly from the true ground and canopy in the point cloud. It also shows potential to identify more detailed plant parts in order to obtain more accurate canopy structural parameters. Future research and more data are required to explore the full potential of this method. For example, whether this method is capable to differentiate between canola cultivars with different architectures and how well this method adapts to other crop species.

Acknowledgments

Trial data were accessed from GRDC project (CSP00169) "Achieving stable and high canola yield across the rainfall ones of WA". The authors would like to thank Sam Flottmann and Adam Brown for field data collection and data assessment and Dr Geoff Bull from High Resolution Plant Phenomics Centre for accessing the LiDAR data.

Disclosure statement

No potential conflict of interest was reported by the authors.

Funding

This work was supported by the Commonwealth Scientific and Industrial Research Organisation.

ORCID

Lian Wu  <http://orcid.org/0000-0001-8973-0058>

References

Alexander, C., K. Tansey, J. Kaduk, D. Holland, and N. J. Tate. 2010. "Backscatter Coefficient as an Attribute for the Classification of Full-Waveform Airborne Laser Scanning Data in Urban Areas." *ISPRS Journal of Photogrammetry and Remote Sensing* 65 (5): 423–432. Elsevier B.V. doi:[10.1016/j.isprsjprs.2010.05.002](https://doi.org/10.1016/j.isprsjprs.2010.05.002).

- Aminpanah, H. 2013. "Effect of Nitrogen Rate on Seed Yield, Protein and Oil Content of Two Canola (*Brassica Napus* L.) Cultivars." *Acta Agriculturae Slovenica* 101 (2): 183–190. doi:10.2478/acas-2013-0014.
- Breiman, L. 2001. "Random Forests." *Machine Learning* 45 (1): 5–32. doi:10.1023/A:1010933404324.
- Calders, K., G. Newnham, A. Burt, S. Murphy, P. Raunonen, M. Herold, D. Culvenor, et al. 2015. "Nondestructive Estimates of Above-Ground Biomass Using Terrestrial Laser Scanning." *Methods in Ecology and Evolution* 6 (2): 198–208. doi:10.1111/2041-210X.12301.
- Colton, R. T., and J. D. Sykes. 1992. *Canola*. 4th ed. Sydney: NSW Agriculture.
- Costes, E., P. E. Lauri, S. Simon, and B. Andrieu. 2013. "Plant Architecture, Its Diversity and Manipulation in Agronomic Conditions, in Relation with Pest and Pathogen Attacks." *European Journal of Plant Pathology* 135 (3): 455–470. doi:10.1007/s10658-012-0158-3.
- Cui, Y., K. Zhao, W. Fan, and X. Xiru. 2011. "Retrieving Crop Fractional Cover and LAI Based on Airborne Lidar Data." *Journal of Remote Sensing* □□□□ 4619 (40734025): 1007–4619.
- Deery, D., J. Jimenez-Berni, H. Jones, X. Sirault, and R. Furbank. 2014. "Proximal Remote Sensing Buggies and Potential Applications for Field-Based Phenotyping." *Agronomy* 4 (3): 349–379. doi:10.3390/agronomy4030349.
- Ducic, V., M. Hollaus, A. Ullrich, W. Wagner, and T. Melzer. 2006. "3D Vegetation Mapping And Classification Using Full-Waveform Laser Scanning." International Workshop 3D Remote Sensing in Forestry, Session 8a (July 2014). pp. 211–217. Vienna.
- Elshkaki, A., E. Der Van Voet, V. Timmermans, and M. V. Holderbeke. 2005. "Dynamic Stock Modelling: A Method for the Identification and Estimation of Future Waste Streams and Emissions Based on past Production and Product Stock Characteristics." *Energy* 30 (8 SPEC. ISS.): 1353–1363. doi:10.1016/j.energy.2004.02.019.
- Friedli, M., N. Kirchgessner, C. Grieder, F. Liebis, M. Mannale, and A. Walter. 2016. "Terrestrial 3D Laser Scanning to Track the Increase in Canopy Height of Both Monocot and Dicot Crop Species under Field Conditions." *Plant Methods*. BioMed Central 12 (1): 1–15. doi:10.1186/s13007-016-0109-7.
- Gerke, M., and J. Xiao. 2014. "Fusion of Airborne Laserscanning Point Clouds and Images for Supervised and Unsupervised Scene Classification." *ISPRS Journal of Photogrammetry and Remote Sensing*. International Society for Photogrammetry and Remote Sensing, Inc. (ISPRS) 87: 78–92. doi:10.1016/j.isprsjprs.2013.10.011.
- Ghatak, A. 2017. *Machine Learning with R*. Singapore: Springer Singapore. doi:10.1007/978-981-10-6808-9.
- Hansen, M., R. Dubayah, and R. Defries. 1996. "Classification Trees: An Alternative to Traditional Land Cover Classifiers." *International Journal of Remote Sensing* 17 (5): 1075–1081. doi:10.1080/01431169608949069.
- <https://www.cloudcompare.org/>. 2018. "CloudCompare." <https://www.cloudcompare.org/>
- Hua, S., B. Cao, B. Zheng, B. Li, and C. Sun. 2016. "Quantitative Evaluation of Influence of PROSTRATE GROWTH 1 Gene on Rice Canopy Structure Based on Three-Dimensional Structure Model." *Field Crops Research*. Elsevier B.V. 194: 65–74. doi:10.1016/j.fcr.2016.05.004.
- Jimenez-Berni, J. A., D. M. Deery, P. Rozas-Larraondo, A. G. Condon, G. J. Rebetzke, R. A. James, W. D. Bovill, R. T. Furbank, and X. R. Sirault. 2018. "High Throughput Determination of Plant Height, Ground Cover and above-Ground Biomass in Wheat with LiDAR." *Frontiers in Plant Science* (February). doi:10.3389/fpls.2018.00237.
- Koenig, K., B. Höfle, L. Müller, M. Hämmerle, T. Jarmer, B. Siegmann, and H. Lilienthal. 2013. "Radiometric Correction of Terrestrial LiDAR Data for Mapping of Harvest Residues Density." *ISPRS Annals of Photogrammetry, Remote Sensing and Spatial Information Sciences* II-5/W2 (November): 133–138. doi:10.5194/isprannals-II-5-W2-133-2013.
- Koenig, K., B. Höfle, M. Hämmerle, T. Jarmer, B. Siegmann, and H. Lilienthal. 2015. "Comparative Classification Analysis of Post-Harvest Growth Detection from Terrestrial LiDAR Point Clouds in Precision Agriculture." *ISPRS Journal of Photogrammetry and Remote Sensing*. International Society for Photogrammetry and Remote Sensing, Inc. (ISPRS) 104 (June): 112–125. doi:10.1016/j.isprsjprs.2015.03.003.

- Korhonen, L., I. Korpela, J. Heiskanen, and M. Maltamo. 2011. "Airborne Discrete-Return LIDAR Data in the Estimation of Vertical Canopy Cover, Angular Canopy Closure and Leaf Area Index." *Remote Sensing of Environment*. Elsevier Inc. 115 (4): 1065–1080. doi:[10.1016/j.rse.2010.12.011](https://doi.org/10.1016/j.rse.2010.12.011).
- Lantz, B. 2015. *Machine Learning with R: Discover How to Build Machine Learning Algorithms, Prepare Data, and Dig Deep into Data Prediction Techniques with R*. 2nd ed. Birmingham: Packt Publishing.
- Lefsky, M. A., W. B. Cohen, D. J. Harding, G. G. Parker, S. A. Acker, and S. Thomas Gower. 2002. "Lidar Remote Sensing of Above-Ground Biomass in Three Biomes." *Global Ecology and Biogeography* 11 (5): 393–399. doi:[10.1046/j.1466-822x.2002.00303.x](https://doi.org/10.1046/j.1466-822x.2002.00303.x).
- Li, W., Z. Niu, C. Wang, W. Huang, H. Chen, S. Gao, L. Dong, and S. Muhammad. 2015. "Combined Use of Airborne LiDAR and Satellite GF-1 Data to Estimate Leaf Area Index, Height, and Aboveground Biomass of Maize during Peak Growing Season." *IEEE Journal of Selected Topics in Applied Earth Observations and Remote Sensing* 8 (9): 4489–4501. doi:[10.1109/JSTARS.2015.2496358](https://doi.org/10.1109/JSTARS.2015.2496358).
- Lim, K., P. Treitz, K. Baldwin, I. Morrison, and J. Green. 2003. "Lidar Remote Sensing of Biophysical Properties of Tolerant Northern Hardwood Forests." *Canadian Journal of Remote Sensing* 29 (5): 658–678. doi:[10.5589/m03-025](https://doi.org/10.5589/m03-025).
- Lindberg, E., J. Holmgren, K. Olofsson, J. Wallerman, and H. Olsson. 2013. "Estimation of Tree Lists from Airborne Laser Scanning Using Tree Model Clustering and K-MSN Imputation." *Remote Sensing* 5 (4): 1932–1955. doi:[10.3390/rs5041932](https://doi.org/10.3390/rs5041932).
- Liu, S., F. Baret, M. Abichou, F. Boudon, S. Thomas, K. Zhao, C. Fournier, et al. 2017. "Estimating Wheat Green Area Index from Ground-Based LiDAR Measurement Using a 3D Canopy Structure Model." *Agricultural and Forest Meteorology* 247 (July): 12–20. Elsevier. doi:[10.1016/j.agrformet.2017.07.007](https://doi.org/10.1016/j.agrformet.2017.07.007).
- Luo, S., C. Wang, X. Xiaohuan, and F. Pan. 2014. "Estimating FPAR of Maize Canopy Using Airborne Discrete-Return LiDAR Data." *Optics Express* 22 (5): 5106. doi:[10.1364/OE.22.005106](https://doi.org/10.1364/OE.22.005106).
- Maddonni, G. A., M. E. Otegui, and A. G. Cirilo. 2001. "Plant Population Density, Row Spacing and Hybrid Effects on Maize Canopy Architecture and Light Attenuation." *Field Crops Research* 71 (3): 183–193. doi:[10.1016/S0378-4290\(01\)00158-7](https://doi.org/10.1016/S0378-4290(01)00158-7).
- McMahon, S. M., D. P. Bebbler, N. Butt, M. Crockatt, K. Kirby, G. G. Parker, T. Riutta, and E. M. Slade. 2015. "Ground Based LiDAR Demonstrates the Legacy of Management History to Canopy Structure and Composition across a Fragmented Temperate Woodland." *Forest Ecology and Management*. Elsevier B.V. 335: 255–260. doi:[10.1016/j.foreco.2014.08.039](https://doi.org/10.1016/j.foreco.2014.08.039).
- Nie, S., C. Wang, P. Dong, and X. Xiaohuan. 2016. "Estimating Leaf Area Index of Maize Using Airborne Discrete-Return Lidar Data." *Remote Sensing Letters* 7 (2): 111–120. doi:[10.1080/2150704X.2015.1111536](https://doi.org/10.1080/2150704X.2015.1111536).
- Omasa, K., F. Hosoi, and A. Konishi. 2006. "3D Lidar Imaging for Detecting and Understanding Plant Responses and Canopy Structure." *Journal of Experimental Botany* 58 (4): 881–898. doi:[10.1093/jxb/erl142](https://doi.org/10.1093/jxb/erl142).
- Pal, M., and P. M. Mather. 2003. "An Assessment of the Effectiveness of Decision Tree Methods for Land Cover Classification." *Remote Sensing of Environment* 86 (4): 554–565. doi:[10.1016/S0034-4257\(03\)00132-9](https://doi.org/10.1016/S0034-4257(03)00132-9).
- Pangga, I. B., J. Hanan, and S. Chakraborty. 2013. "Climate Change Impacts on Plant Canopy Architecture: Implications for Pest and Pathogen Management." *European Journal of Plant Pathology* 135 (3): 595–610. doi:[10.1007/s10658-012-0118-y](https://doi.org/10.1007/s10658-012-0118-y).
- Raumonen, P., M. Kaasalainen, M. Åkerblom, S. Kaasalainen, H. Kaartinen, M. Vastaranta, M. Holopainen, M. Disney, and P. Lewis. 2013. "Fast Automatic Precision Tree Models from Terrestrial Laser Scanner Data." *Remote Sensing* 5 (2): 491–520. doi:[10.3390/rs5020491](https://doi.org/10.3390/rs5020491).
- Richardson, J. J., L. M. Moskal, and S. H. Kim. 2009. "Modeling Approaches to Estimate Effective Leaf Area Index from Aerial Discrete-Return LIDAR." *Agricultural and Forest Meteorology* 149 (6–7): 1152–1160. doi:[10.1016/j.agrformet.2009.02.007](https://doi.org/10.1016/j.agrformet.2009.02.007).

- Rutzinger, M., B. Höfle, M. Hollaus, and N. Pfeifer. 2008. "Object-Based Point Cloud Analysis of Full-Waveform Airborne Laser Scanning Data for Urban Vegetation Classification." *Sensors* 8 (8): 4505–4528. doi:[10.3390/s8084505](https://doi.org/10.3390/s8084505).
- Sankaran, S., L. R. Khot, and A. H. Carter. 2015. "Field-Based Crop Phenotyping: Multispectral Aerial Imaging for Evaluation of Winter Wheat Emergence and Spring Stand." *Computers and Electronics in Agriculture*. Elsevier B.V. 118 (October): 372–379. doi:[10.1016/j.compag.2015.09.001](https://doi.org/10.1016/j.compag.2015.09.001).
- Solberg, S., E. Næsset, K. H. Hanssen, and E. Christiansen. 2006. "Mapping Defoliation during a Severe Insect Attack on Scots Pine Using Airborne Laser Scanning." *Remote Sensing of Environment* 102 (3–4): 364–376. doi:[10.1016/j.rse.2006.03.001](https://doi.org/10.1016/j.rse.2006.03.001).
- Vauhkonen, J., L. Ene, S. Gupta, J. Heinzel, J. Holmgren, J. Pitkänen, S. Solberg, et al. 2012. "Comparative Testing of Single-Tree Detection Algorithms under Different Types of Forest." *Forestry* 85 (1): 27–40. doi:[10.1093/forestry/cpr051](https://doi.org/10.1093/forestry/cpr051).
- Wu, W., L. Nie, F. Shah, Y. Liao, K. Cui, D. Jiang, J. Xie, Y. Chen, and J. Huang. 2014. "Influence of Canopy Structure on Sheath Blight Epidemics in Rice." *Plant Pathology* 63 (1): 98–108. doi:[10.1111/ppa.12078](https://doi.org/10.1111/ppa.12078).
- Zhao, K., M. García, S. Liu, Q. Guo, G. Chen, X. Zhang, Y. Zhou, and X. Meng. 2015. "Terrestrial Lidar Remote Sensing of Forests: Maximum Likelihood Estimates of Canopy Profile, Leaf Area Index, and Leaf Angle Distribution." *Agricultural and Forest Meteorology*. Elsevier B.V. 209–210: 100–113. doi:[10.1016/j.agrformet.2015.03.008](https://doi.org/10.1016/j.agrformet.2015.03.008).
- Zhao, K., S. Popescu, X. Meng, Y. Pang, and M. Agca. 2011. "Characterizing Forest Canopy Structure with Lidar Composite Metrics and Machine Learning." *Remote Sensing of Environment*. Elsevier Inc. 115 (8): 1978–1996. doi:[10.1016/j.rse.2011.04.001](https://doi.org/10.1016/j.rse.2011.04.001).
- Zhao, Y., Y. Ming, X. Liu, E. Zhu, K. Zhao, and J. Yin. 2018. "Large-Scale k-Means Clustering via Variance Reduction." *Neurocomputing*. Elsevier B.V. 307 (September): 184–194. doi:[10.1016/j.neucom.2018.03.059](https://doi.org/10.1016/j.neucom.2018.03.059).
- Zlinszky, A., W. Mücke, H. Lehner, C. Briese, and N. Pfeifer. 2012. "Categorizing Wetland Vegetation by Airborne Laser Scanning on Lake Balaton and Kis-Balaton, Hungary." *Remote Sensing* 4 (6): 1617–1650. doi:[10.3390/rs4061617](https://doi.org/10.3390/rs4061617).